

LETTER TO THE EDITOR

Lutetium and Oxygen Displacements in Orthorhombic T' -Type $\text{Lu}_2\text{PdO}_{4-\delta}$

Bai-Hao Chen and David Walker

Lamont–Doherty Earth Observatory of Columbia University, Palisades, New York 10964

Communicated by J. B. Goodenough April 21, 1997; accepted April 21, 1997

Lutetium palladium oxide, $\text{Lu}_2\text{PdO}_{4-\delta}$, has been prepared in a multianvil apparatus at 60 kbar pressure and 1100°C. It crystallizes in an orthorhombic T' (Nd_2CuO_4)-type structure with the space group $Pbca$ (No. 61), $a = 5.479(1)$ Å, $b = 5.501(1)$ Å, $c = 11.579(2)$ Å, $V = 349.0$ Å³, and $Z = 4$. Lutetium and oxygen displacements in the new phase create sixfold coordination for Lu, relieve the compressive stress on the Pd–O bonds resulting from the geometrical mismatch between the PdO_2 and Lu_2O_2 layers, and reduce the electrostatic repulsion between oxygens. © 1997 Academic Press

Crystal chemistry plays a dominant role in determining the doping preferences in Ln_2CuO_4 ($\text{Ln} = \text{rare earth}$) cuprates. As pointed out by Goodenough (1), the geometrical mismatch between the CuO_2 sheets and Ln_2O_2 fluorite-type layers along the c -axis in these intergrowth phases creates a stress on the Cu–O bonds. The T (K_2NiF_4)-type cuprates with compressive Cu–O bonds are p -type superconductors, while the T' (Nd_2CuO_4)-type cuprates with tensile Cu–O bonds are n -type superconductors. However, the tensile stress on the Cu–O bonds decreases with the size of the Ln cations, finally reversing to compressive stress as found in orthorhombic Gd_2CuO_4 by Braden *et al.* (2). This leads to the bending of the Cu–O–Cu angles from 180° (i.e., oxygen displacement). Unsurprisingly, the (Gd, M) $_2\text{CuO}_4$ ($\text{M} = \text{Ce}$ and Th) phases are not superconducting. In addition to oxygen displacements, evidence of cation displacements in Y_2CuO_4 and Tm_2CuO_4 phases has been found by Bordet *et al.* based on electron diffraction (3). However, the structure has not been solved, leaving the nature of the cation displacements unclear.

The stability ranges of the T and T' phases have been extensively investigated in the past few years using Goldschmidt's tolerance factor (i.e., the perovskite tolerance factor), $t = (r_A + r_O)/\sqrt{2}(r_B + r_O)$ (4, 5). Recently, a tolerance factor for the Nd_2CuO_4 -type structure, $\text{tf} = [3\sqrt{2}r_O +$

$2\sqrt{6}(r_A + r_O)]/9(r_B + r_O)$, has also been introduced (6). Using Shannon's crystal radii (7), it is found that T' phases occur for $\text{tf} < 1.00$ while T phases form for $\text{tf} > 1.00$. Many ternary compounds, including oxides, sulfides, and halides, crystallize in the T -type structure (8, 9). In contrast, there is less known about the T' -type phases, which include Ln_2CuO_4 ($\text{Ln} = \text{Y}, \text{Nd–Tm}$) cuprates and R_2PdO_4 ($\text{R} = \text{La}$ and Nd) palladates (10–13). However, single phases of palladates have not yet been obtained and their structure has not been well established. We have recently investigated the phase stability of the T' -type palladates and discovered a new $\text{Lu}_2\text{PdO}_{4-\delta}$ phase.

The title compound was synthesized from a mixture of elemental Pd and Lu_2O_3 with KClO_3 as an oxygen source in the molar ratio 3:3:1 in a multianvil apparatus at 60 kbar and 1100°C for 1 h, using an Al_2O_3 capsule. A full description of the multianvil apparatus and the high-pressure experimental procedures has been published previously (14, 15). The composition of the title compound was determined with a CAMEBAX electron microprobe to be $\text{Lu}_2\text{PdO}_{3.8(1)}$. B -type Lu_2O_3 and Pd metal were used as standards for Lu and O and for Pd, respectively.

The X-ray powder diffraction data were collected with a Siemens D-500 diffractometer using $\text{CuK}\alpha$ radiation at room temperature in the range $10^\circ < 2\theta < 80^\circ$ with a step width of 0.02° and a counting period of 20 s. Although the X-ray pattern is similar to that of the T' -type cuprates, several reflections at the 2θ values $27.6^\circ, 33.5^\circ, 38.8^\circ, 47.5^\circ, 51.5^\circ, 55.1^\circ, 62.3^\circ$, and 75.2° were unidentified. However, these can be indexed on an orthorhombic superstructure with $a \sim \sqrt{2}a_1$, $b \sim \sqrt{2}a_1$, and $c \sim c_1$, where the subscript t refers to the tetragonal (regular) T' -type structure. The systematic absence of $0kl$: $k = 2n + 1$, $h0l$: $l = 2n + 1$, $hk0$: $h = 2n + 1$, $h00$: $h = 2n + 1$, $0k0$: $k = 2n + 1$, $00l$: $l = 2n + 1$ suggests that the structure belongs to the space group $Pbca$. Thus, an orthorhombic T' -type model with the $Pbca$ space group was proposed and was refined by a Rietveld profile analysis of X-ray powder diffraction data with

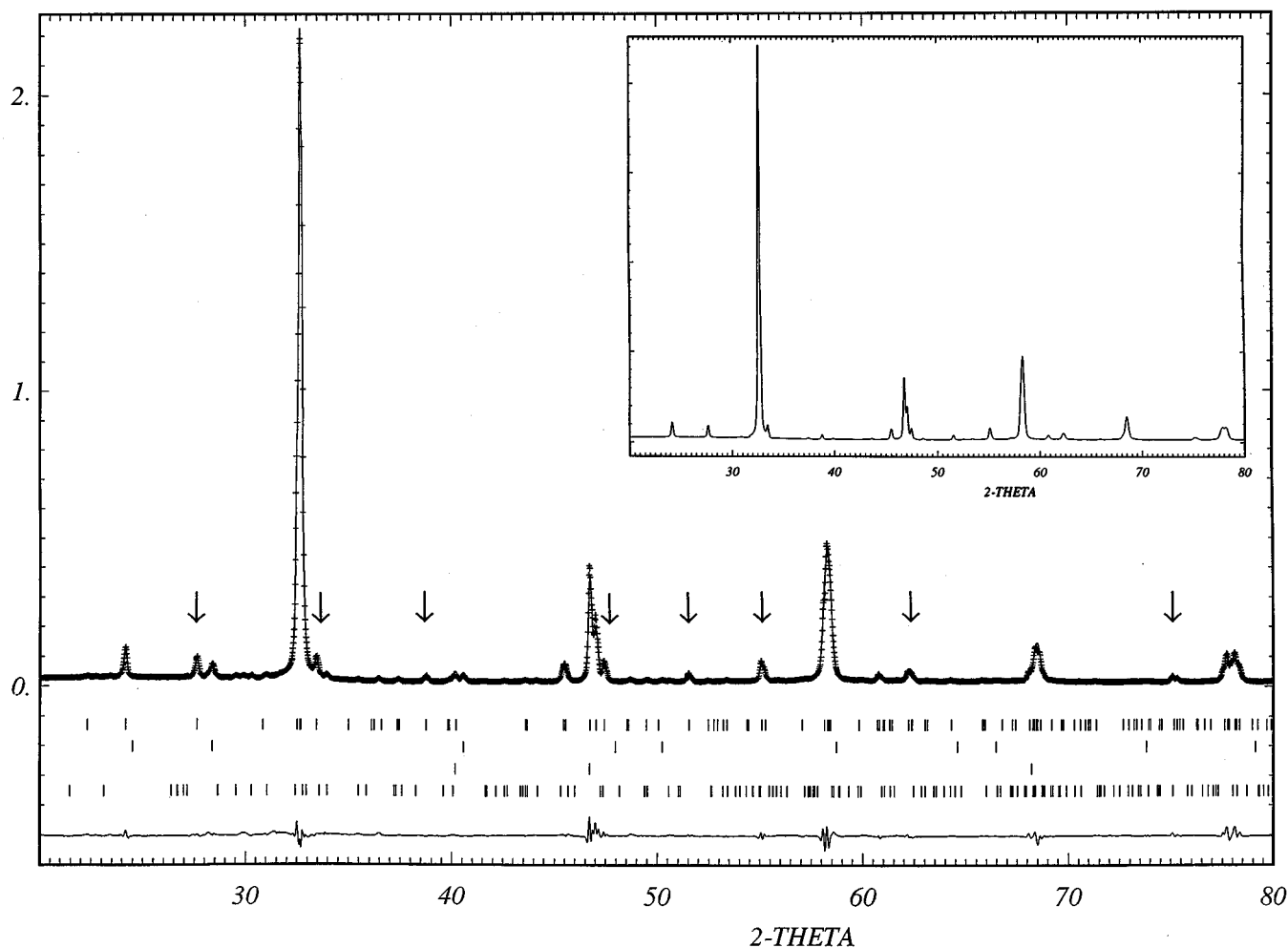


FIG. 1. Comparison of calculated (solid line) and observed (dots) X-ray patterns for Lu_2PdO_4 and other components. Locations of calculated reflections (vertical tick marks) from the top to the bottom associate with Lu_2PdO_4 , KCl, Pd, and Lu_2O_3 . Difference (bottom curve) between calculated and observed patterns. Reflections corresponding to the superstructure are marked by arrows. The calculated pattern for Lu_2PdO_4 is shown in the insert.

the FULLPROF program (16). The total number of reflections is 109. The refined parameters include lattice parameters, atomic positions, isotropic thermal parameters, a zero-point error, overall scale factor, background, parameter of a pseudo-Voigt peak-shape function, and half-width parameters. Because the refinement of any occupancy cannot improve the R factors, all occupancies were fixed at 1 in the final refinement. Small amounts of the impurity phases Pd, KCl, and B -type Lu_2O_3 in the sample were also included in the refinement. The final R factors are $R_p = 5.48\%$, $R_{wp} = 7.64\%$, $R_b = 3.35\%$, and $R_e = 1.53\%$ (17). The crystallographic data are summarized in Table 1. A comparison of calculated and observed X-ray patterns is shown in Fig. 1. The structure of the title compound is presented in Fig. 2. Lutetium and oxygen displacements in the title compound with respect to the Nd_2CuO_4 -type structure are shown in Fig. 3.

The title compound, like Nd_2CuO_4 , consists of an intergrowth of PdO_2 layers and Lu_2O_2 fluorite-type slabs along the c -axis. However, the orthorhombic distortion leads to lutetium and oxygen displacements. The adjacent square planar PdO_4 groups rotate toward each other about axes slightly tilted to the c -axis. Such oxygen displacements not only relieve the compressive stress on the Pd–O bonds but also reduce the coordination number of Lu from eight in the regular T' -type to six. The oxygen arrangement in LuO_6 , similar to that in C -type Lu_2O_3 (18), can be derived by moving two oxygen atoms at the ends of a face-diagonal of a LuO_8 cube away from Lu as a result of the rotation of the PdO_4 groups. In fact, Lu coordinated by six oxygens is most common in oxides (18–20). In addition, the Lu_2O_2 slabs shift alternatively in the b and $-b$ directions with respect to those of the regular T' -type (see Fig. 3). Furthermore, O_a (oxygen in the PdO_2 layers) ions are coordinated by two Lu

TABLE 1
Crystallographic Data for Lu_2PdO_4 with Estimated Standard Deviations in Parentheses

Atom	Site	Positional and isotropic thermal parameters			$B(\text{\AA}^2)$
		x	y	z	
Lu	8c	-0.0073(6)	0.0361(4)	0.3414(3)	3.2(1)
Pd	4a	0	0	0	2.5(1)
Oa	8c	0.176(3)	0.324(3)	0.007(2)	2.0(7)
Ob	8c	0.243(3)	0.271(3)	0.282(2)	3.8(9)
Selected bond lengths (\AA) and angles ($^\circ$)					
Lu-Oa	2.30(2)	Lu-Ob	2.01(2)	Pd-Oa	2.03(1) $\times 2$
Lu-Oa	2.31(2)	Lu-Ob	2.17(2)	Pd-Oa	2.02(1) $\times 2$
Lu...Oa	2.93(2)	Lu-Ob	2.36(2)		
Lu...Oa	3.30(2)	Lu-Ob	2.41(2)		
Oa-Oa	2.87(2) $\times 2$	Ob-Ob	2.75(2) $\times 2$	Oa-Ob	3.22(2)
Oa-Oa	2.86(2) $\times 2$	Ob-Ob	2.84(2) $\times 2$	Oa-Ob	2.68(2)
Oa-Oa	2.74(2)				
O-Pd-O	89.9(1)	O-Pd-O	90.1(1)	Pd-O-Pd	146.9(2)

Note. Space group $Pbca$ (No. 61), $a = 5.479(1) \text{\AA}$, $b = 5.501(1) \text{\AA}$, $c = 11.579(2) \text{\AA}$, and $Z = 4$.

and two Pd cations, forming $(\text{Lu}_2\text{Pd}_2)\text{O}$ pseudo-tetrahedra. In contrast, Nd_2CuO_4 consists of *trans*- $(\text{Nd}_4\text{Cu}_2)\text{O}$ octahedra.

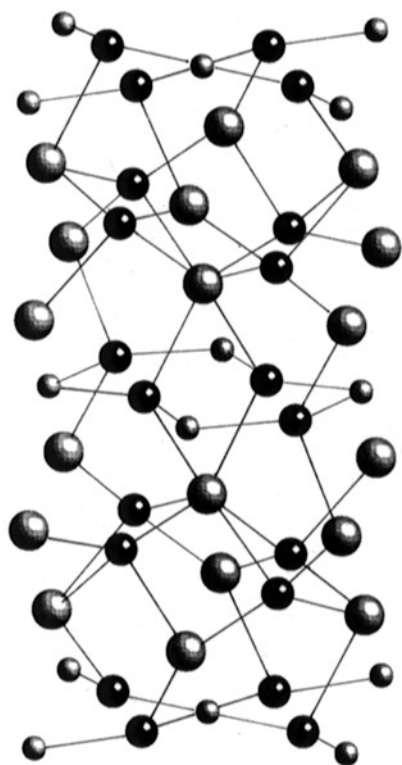


FIG. 2. Crystal structure of Lu_2PdO_4 , showing square planar PdO_4 groups, LuO_6 polyhedra, and $(\text{Lu}_2\text{Pd}_2)\text{O}$ pseudo-tetrahedra. The large, small, and medium (black) spheres represent Lu, Pd, and O, respectively.

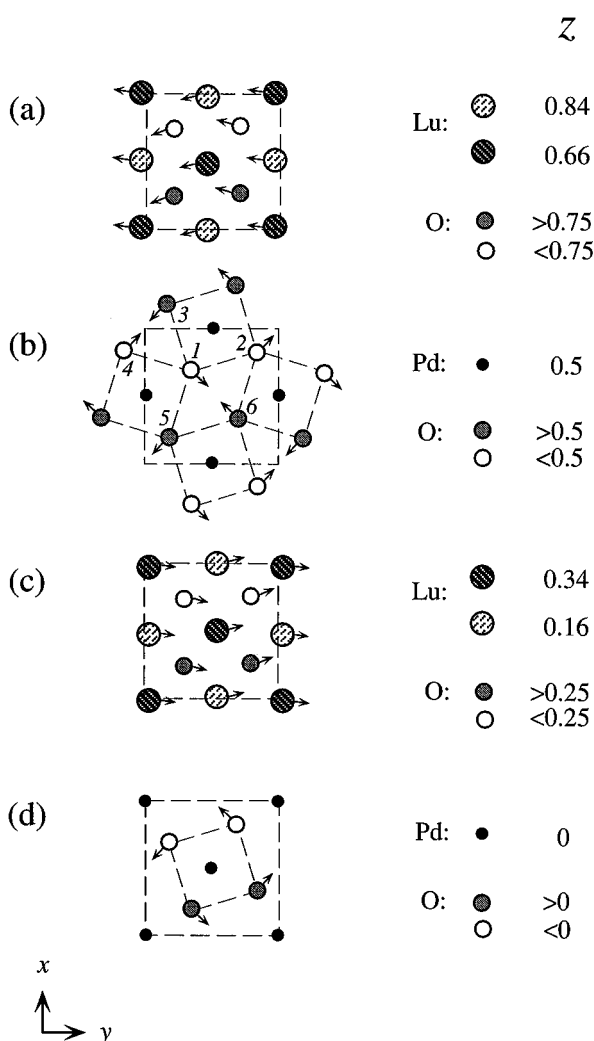


FIG. 3. Lutetium and oxygen displacements in the Lu_2PdO_4 -type with respect to those of the Nd_2CuO_4 -type. Directions of displacements are shown by arrows. Distance between Oa1 and Oa6 decreases with an increase in the rotation of the PdO_4 groups shown in (b).

The orthorhombic distortion also leads to the formation of buckled PdO_2 layers. In the case of the regular T' -type, each oxygen (Oa1) is surrounded by four equidistant oxygens in the BO_2 layers. In the case of the title compound, the rotation of the PdO_4 groups creates the fifth oxygen neighbor (Oa6) of Oa1 (see Fig. 3b). At a rotation greater than 15° , assuming that all O-Pd-O angles are 90° and all Pd-O distances are the same, the Oa1-Oa6 distances become the shortest Oa-Oa distances. The rotation in the title compound is about 16.5° . Unsurprisingly, the strong electron repulsion between the oxygens causes buckling of the PdO_2 layers.

The average Pd-O bond distance of 2.02\AA is the same as that calculated using Shannon's ionic radii, but much longer than that of 1.94\AA based on the regular T' model. The average of the first-nearest six Lu-O bond distances of

TABLE 2
Comparison Among the T' -Type A_2BO_4 Structures

Structural type	Nd ₂ CuO ₄	Gd ₂ CuO ₄	Lu ₂ PdO ₄
Crystal system	Tetragonal	Orthorhombic	Orthorhombic
Space group	$I4/mmm$ (No. 139)	$Abcm$ (No. 64)	$Pbca$ (No. 61)
Unit cell dim.	$a_1 \times a_1 \times c_1$	$\sqrt{2}a_1 \times \sqrt{2}a_1 \times c_1$	$\sqrt{2}a_1 \times \sqrt{2}a_1 \times c_1$
Displacements	No	Oa	A, Oa, and Ob
A coordinated by	4 Oa and 4 Ob	4 Oa and 4 Ob	2 Oa and 4 Ob
Oa coordinated by	4 A and 2 B	4 A and 2 B	2 A and 2 B
BO ₂ layer shape	Flat	Flat	Buckled
B–O–B angle (°)	180	170	147

Note. Oa, oxygen anions in BO₂ layers. Ob, oxygen anions in A₂O₂ layers.

2.26 Å is also similar to that calculated from Shannon's ionic radii, 2.24 Å. The seventh (2.93 Å) and eighth Lu–O distances (3.30 Å) are much greater than the average of the first-nearest six Lu–O distances, indicating that they are second- and third-nearest neighbors of Lu. The average Oa–Oa and Ob–Ob distances are 2.84 and 2.80 Å, respectively, compared to that of 2.74 Å calculated using the regular T' -model, suggesting that the oxygen displacements can reduce the electrostatic repulsion between oxygens. The Pd–O–Pd bond angle is 147°, compared to 180° in the regular T' -model.

The crystal chemistry of the T' -type A_2BO_4 structures exhibits very interesting features. Table 2 compares these structures. The replacement of Nd by small rare earth cations results in transitions from the tetragonal ($I4/mmm$) Nd₂CuO₄-type to the orthorhombic ($Abcm$) Gd₂CuO₄-type (2) and finally to the orthorhombic ($Pbca$) Lu₂PdO₄-type structure. In the case of the Nd₂CuO₄-type cuprates with large rare earths, the Cu–O bond distances decrease from 1.98 Å for Pr₂CuO₄ to 1.96 Å for Eu₂CuO₄, suggesting that the Cu–O bonds are under tension. In the case of the Gd₂CuO₄-type cuprates with intermediate rare earths, the Cu–O bond distances remain constant at 1.95 Å. However, the compression on the Cu–O bonds leads to oxygen displacements by rotation of the square planar CuO₄ about the c -axis. In the case of the Lu₂PdO₄-type phase with small rare earths, the major driving force of oxygen displacements is the presence of the sixfold-coordinated rare earth cations in conjunction with the geometrical mismatch between the A₂O₂ and BO₂ layers. In addition, the electrostatic repulsion between oxygens is also a factor. Such a large distortion leads to cation displacements. As mentioned previously, the observation of cation displacements in Y₂CuO₄ and Tm₂CuO₄ suggests that they might have a Lu₂PdO₄-related structure (3).

The tolerance factor tf values in Ref. 6 were calculated using Shannon's crystal radii (7), which give the O–O bond

distance of 2.52 Å. This study shows that the O–O distances are similar to that of 2.80 Å calculated using effective ionic radii (21), suggesting the latter should be employed for computing tf . Thus, the T and T' phases are separated at $tf = 1.035$ rather than at 1.00 as reported in Ref. 6. The discovery of Lu₂PdO_{4– δ} extends the lower limit of tf to 0.958.

ACKNOWLEDGMENTS

The authors thank Dr. B. A. Scott for helpful discussions and Ms. J. Hanley for technical assistance. This work is contribution 5656 from the Lamont–Doherty Earth Observatory of Columbia University and was supported by the National Science Foundation.

REFERENCES

1. J. B. Goodenough, *Supercond. Sci. Technol.* **3**, 26 (1990).
2. M. Braden, W. Paulus, A. Cousson, P. Vigoureux, G. Heger, A. Goukassov, P. Bourges, and D. Petitgrand, *Europhys. Lett.* **25**, 625 (1994).
3. P. Bordet, J. J. Capponi, C. Chaillout, D. Chateigner, J. Chenavas, Th. Fournier, J. L. Hodeau, M. Marrezio, M. Perroux, G. Thomas, and A. Varela, *Physica C* **193**, 178 (1992).
4. J. B. Goodenough and A. Manthiram, *J. Solid State Chem.* **88**, 115 (1990).
5. J. F. Bringley, S. S. Trail, and B. A. Scott, *J. Solid State Chem.* **86**, 310 (1990).
6. B.-H. Chen, *J. Solid State Chem.* **125**, 63 (1996).
7. R. D. Shannon, *Acta Crystallogr. A* **32**, 751 (1976).
8. O. Muller and R. Roy, "The Major Ternary Structural Families." Springer-Verlag, Berlin, 1974.
9. B.-H. Chen and B. W. Eichhorn, *Mater. Res. Bull.* **26**, 1035 (1991); M. Saeki, Y. Yajima, and M. Onoda, *J. Solid State Chem.* **92**, 286 (1991).
10. Hk. Müller-Buschbraum and W. Wollschläger, *Z. Anorg. Allg. Chem.* **414**, 76 (1975).
11. H. Okada, M. Takano, and Y. Takeda, *Physica C* **166**, 111 (1990). [See references therein.]
12. (a) B. G. Kakhan, V. B. Lazarev, and I. S. Shaplygin, *Russ. J. Inorg. Chem.* **27**, 1180 (1982) [Engl. Transl.]; (b) B. G. Kakhan, V. B. Lazarev, and I. S. Shaplygin, *Russ. J. Inorg. Chem.* **27**, 1352 (1982). [Engl. Transl.]
13. J. P. Attfield and G. Férey, *J. Solid State Chem.* **80**, 286 (1989).
14. D. Walker, *Am. Miner.* **76**, 1092 (1991).
15. B.-H. Chen, D. Walker, E. Suard, B. Scott, B. Mercey, M. Hervieu, and B. Raveau, *Inorg. Chem.* **34**, 2077 (1995).
16. J. Rodriguez-Carvajal, in "Abstracts of the Satellite Meeting on Powder Diffraction of the XV Congress of the International Union of Crystallography, Toulouse, France, 1990," p. 127.
17. R. A. Young and D. B. Wiles, *J. Appl. Crystallogr.* **15**, 430 (1982).
18. A. F. Wells, "Structural Inorganic Chemistry," 5th ed., pp. 543–547. Clarendon, Oxford, 1984.
19. H.-R. Freund and Hk. Müller-Buschbraum, *Z. Naturforsch. B* **32**, 1123 (1977).
20. M. Marrezio, J. P. Remeika, and P. D. Dernier, *Acta Crystallogr. B* **26**, 2008 (1970).
21. R. D. Shannon and C. T. Prewitt, *Acta Crystallogr. B* **25**, 925 (1969).